Efficient Photoredox Cycles to Control Perylenediimide Self-Assembly

Chunfeng Chen, Jorge Santos Valera, Takuji B. M. Adachi, Thomas Hermans

Chemistry Europe
European Chemical Societies Publishing

WILEY VCH

Excellence in Chemistry Research

Announcing our new flagship journal

- Gold Open Access
- Publishing charges waived
- Preprints welcome
- Edited by active scientists

Meet the Editors of *ChemistryEurope*

Luisa De Cola
Università degli Studi di Milano Statale, Italy

Ive Hermans
University of Wisconsin-Madison, USA

Ken Tanaka
Tokyo Institute of Technology, Japan

Chemistry–A European Journal
Research Article
doi.org/10.1002/chem.202202849
Chemistry Europe
European Chemical Societies Publishing
www.chemeurj.org

Efficient Photoredox Cycles to Control Perylenediimide Self-Assembly**

Chunfeng Chen,[a] Jorge S. Valera,[a] Takuji B. M. Adachi,[b] and Thomas M. Hermans*[a]

Abstract: Photoreduction of perylenediimide (PDI) derivatives has been widely studied for use in photocatalysis, hydrogen evolution, photo-responsive gels, and organic semiconductors. Upon light irradiation, the radical anion ($PDI^{\bullet-}$) can readily be obtained, whereas further reduction to the dianion (PDI^{2-}) is rare. Here we show that full 2-electron photoreduction can be achieved using UVC light: 1) in anaerobic conditions by 'direct photoreduction' of PDI aggregates, or 2) by 'indirect photoreduction' in aerobic conditions due to acetone ketyl radicals. The latter strategy is also efficient for other dyes, such as naphthalenediimide (NDI) and methylviologen (MV^{2+}). Efficient photoreduction on the minute time-scale using simple LED light in aerobic conditions is attractive for use in dissipative light-driven systems and materials.

Introduction

Perylenediimides (PDIs) are well-known dyes with outstanding properties, such as photo-thermal stability[1] and high electron mobility.[2] Specifically, their electron-poor character renders them excellent electron acceptors that can produce stable radical anions.[3] These properties make PDIs promising materials as organic electron-transporting materials (by electron-hole transfer),[4–8] for water splitting (by electron-transfer),[9,10] as near-infrared absorber in photothermal therapy,[11–14] or as photocatalysts.[15,16] In an example of the latter, König and co-workers showed that a PDI derivative could reduce aryl halides under inert conditions in DMF or DMSO upon photoexcitation of the radical anion state ($PDI^{\bullet-}$),[15] though the exact mechanism remains under debate.[17] Further reduction of $PDI^{\bullet-}$ to PDI^{2-} has so far only been achieved by chemical ($Na_2S_2O_4$)[18,19] or electrochemical[20–23] means. In addition, both PDI^{2-} and $PDI^{\bullet-}$ quickly oxidize if the solution is exposed to air. An exception to this was shown by the group of Würthner that was able to achieve air-stable zwitterionic[24] or dianionic[25] PDIs using electron-withdrawing bay substitutions. Thus, finding alternative routes to (photo)generate and stabilize PDI^{2-} in open air would be desirable given its promising usefulness in photocatalysis[26,27] and organic electronic devices.[28]

Recently, PDIs have gained attention as building blocks to control dissipative self-assembly, where neutral PDI is the 'activated monomer' that aggregates in aqueous solutions, whereas 'deactivated monomer' PDI^{2-} disassembles due to electrostatic repulsion.[18,29] For example, the fine control of the chemical reduction rate with $Na_2S_2O_4$ and the oxidation rate by oxygen in the air led us to discover interesting behaviors, such as supramolecular oscillations or frontal polymerization.[29] Now, if the chemical reduction step could be replaced by photoreduction, unprecedented spatiotemporal control of dissipative self-assembly could be envisioned, bringing us one step closer to life-like materials.[30] Therefore we set out to achieve efficient and full (2-electron) photoreduction of PDIs under ambient conditions to avoid tedious and time-consuming freeze-pump-thaw cycles.

In studying the 'direct photoreduction' of a PDI derivative – via photoexcited PDI* – we achieve complete reduction of PDI to dianion PDI^{2-} in anaerobic conditions in contrast to previous studies.[15,16] As will be discussed, the reduction process is facilitated by self-assembly. In addition, by screening different solvent conditions we found that acetone catalyzes fast photoreduction to PDI^{2-} even in open-to-air conditions. This 'indirect photoreduction' – via photoexcited acetone* – had previously been explored to reduce azo-dyes[31,32] or graphene oxide[33] under vacuum conditions, but we find it works in air as well. Our strategy also works for other dyes, such as NDI's and MV^{2+}, paving the way towards its application in light-controlled self-assembly processes.

Results and Discussion

First, we synthesized **PDI-1** (Figure 1A, according to Ref. [18]) that we previously[18,29] showed to form micron-sized colloidal

[a] Dr. C. Chen, Dr. J. S. Valera, Prof. T. M. Hermans
Université de Strasbourg, CNRS, UMR7140
4 Rue Blaise Pascal, 67081 Strasbourg (France)
E-mail: hermans@unistra.fr

[b] Prof. T. B. M. Adachi
Department of Physical chemistry Sciences II,
30 Quai Ernest Ansermet
1211, Genève 4 (Switzerland)

[**] A previous version of this manuscript has been deposited on a preprint server (https://doi.org/10.26434/chemrxiv-2022-3lsjg-v2).

Supporting information for this article is available on the WWW under https://doi.org/10.1002/chem.202202849

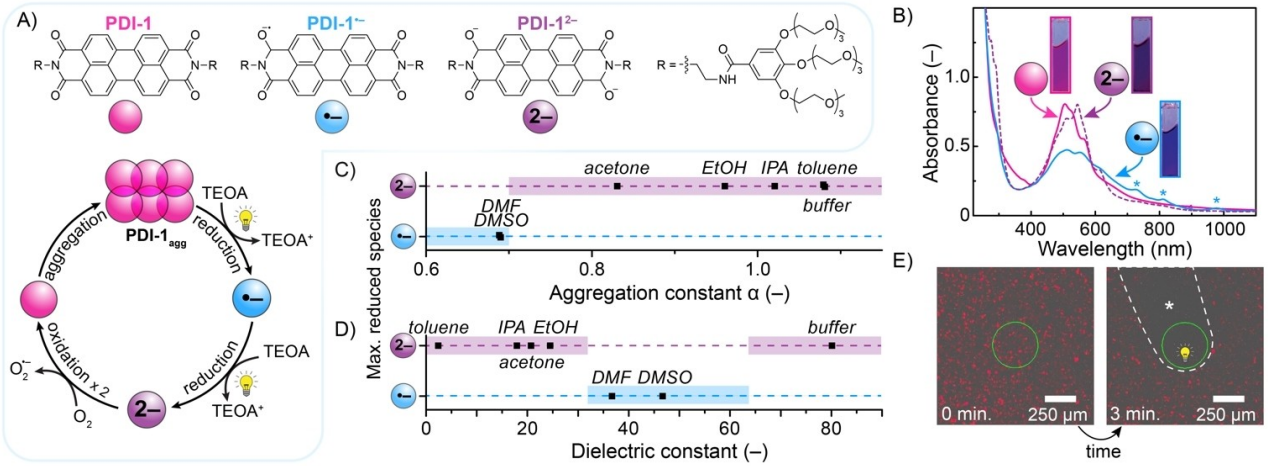

Figure 1. Photoreduction under anaerobic conditions followed by aerobic oxidation. A) The molecular structure of monomeric **PDI-1** (pink), single reduced **PDI-1**$^{\bullet-}$ that photoreduces and disassembles to **PDI-1**$^{\bullet-}$ and upon further illumination to **PDI-1**$^{2-}$. Exposure to air oxidizes **PDI-1**$^{2-}$ to **PDI-1**, followed by re-assembly into **PDI-1**$_{agg}$. **B)** UV-vis spectra of the **PDI-1**$_{agg}$ (33 µM + 3000 eq. TEOA, pink curve) in deoxygenated sodium bicarbonate-carbonate buffer. Upon UVC LED (275 nm, 1 × 8200 mW/m^2) illumination it first forms **PDI-1**$^{\bullet-}$ (blue curve) and then **PDI-1**$^{2-}$ (purple dashed curve). **C)** Maximum reduced species (1 e$^-$ or 2 e$^-$ reduction) versus aggregation constant α. **D)** Maximum reduced species in different solvents; from low to high dielectric constant: toluene, isopropanol, acetone, ethanol, DMF, DMSO, buffer. **E)** Confocal micrographs (overlay of transmitted light and fluorescence with pseudo-colour red) of a degassed 33 µM **PDI-1**$_{agg}$ solution + 3000 eq. of TEOA. After 3 minutes irradiation at the central green circle (355 nm laser) the **PDI-1**$_{agg}$ assemblies are reduced and disassemble in the region indicated with the asterisk (see Supporting Video S1).

aggregates **PDI-1**$_{agg}$ in aqueous buffer. In the current work we use a bicarbonate-carbonate buffer (50 mM) at pH 10.8. Upon illumination under anaerobic conditions, one electron is transferred from the sacrificial electron donor triethanolamine (TEOA) to first yield the singly reduced **PDI-1**$^{\bullet-}$, followed by the doubly reduced **PDI-1**$^{2-}$ (see cycle in Figure 1A). The latter stays reduced indefinitely in the absence of oxygen. However, breaking the vacuum of the cuvette and gentle shaking leads to oxidation (2×) back to neutral **PDI-1**, which assembles into **PDI-1**$_{agg}$ (see Figure 1A cycle). The relevant species **PDI-1**$_{agg}$, **PDI-1**$^{\bullet-}$ and **PDI-1**$^{2-}$ can be easily distinguished by eye as the solutions are pink, blue, and purple, respectively (see insets in Figure 1B), and each species was characterized by UV-Vis spectrometry (Figure 1B).[18,29] **PDI-1**$_{agg}$ shows a broad 400–650 nm absorption with peaks at 528, 505 nm, and 473 nm corresponding to the 0–0, 0–1, 0–2 transitions (pink curve in Figure 1B). In addition, two features support the formation of aggregates. The first is an aggregation band[34,35] at 565 nm, which is absent in the monomeric state (see Figure S1 for **PDI-1** in DMF with well-defined vibronic bands). The second is the shape of the vibronic progressions where for monomeric PDIs the 0–0 absorption is greater than the 0–1 one, whereas for **PDI-1**$_{agg}$ it is the reverse (see annotations in Figure S1). **PDI-1**$^{\bullet-}$ shows three distinct absorption peaks of the radical ion at 723, 809, and 977 nm, in addition to 0–0 and 0–1 transitions at 550 and 512 nm. The spectrum remains broad indicating that **PDI-1**$^{\bullet-}$ is still assembled to some extent.[4] **PDI-1**$^{2-}$, has absorption peaks at 510 and 544 nm and 610 nm, and the 0–0 transition is greater than 0–1.

In the first set of experiments we explored the most suitable wavelength (see Figure S2A) and intensities of light to achieve full photoreduction: blue lamps (390–480 nm, 10 lamps each with power 402 mW/m^2), UVA lamps (316–400 nm, 10 × 1422 mW/m^2), UVB lamps (270–370 nm, 10 × 227.5 mW/m^2), UVC lamps (250–256 nm, 10 × 184.5 mW/m^2) or UVC LED arrays (260–300 nm, 1 or 2 arrays of each 8200 mW/m^2). Using blue or UVA lamps we could only reach the singly reduced **PDI-1**$^{\bullet-}$ (see Figure S2B) even after 1 h of continuous illumination in a vacuum sealed cuvette. However, using the shorter wavelength UVC illumination, full reduction to **PDI-1**$^{2-}$ is achieved within 5 minutes. The UVC illumination is absorbed by higher order $S_0 \rightarrow S_n$ ($n > 2$) PDI transitions,[36] which is the first, but not the only (see below), requirement to achieve efficient photoreduction. All further experiments from here onwards are therefore performed with UVC LED light only.

The second important aspect is whether we have **PDI-1** monomers or **PDI-1**$_{agg}$ aggregates in solution. We quantify the degree of aggregation α by taking the ratio of UV-Vis intensities of the 0–0 versus the 0–1 absorptions, i.e., $\alpha = I_{0-0} / I_{0-1}$, commonly used in the literature to tell the monomer ($\alpha < 0.7$) and aggregates apart ($\alpha > 0.7$).[34,37,38] For **PDI-1**$_{agg}$ (33 µM in carbonate buffer) we find $\alpha = 1.08$. In trying a range of solvents, we observed monomeric states only in dimethylformamide (DMF) and dimethylsulfoxide (DMSO), and aggregates for acetone, ethanol (EtOH), isopropanol (IPA), and toluene (see α values in Figure 1C and all UV-Vis spectra in Figure S3 and exact values in Table S1). Surprisingly, we only reached **PDI-1**$^{\bullet-}$ for monomer solutions (Figure 1C, blue area), whereas **PDI-1**$^{2-}$ was obtained for all **PDI-1**$_{agg}$ solutions (purple area), upon UVC illumination. We exclude the influence of the dielectric constant of the solvent, as no trend can be discerned in Figure 1D, whereas it is clear that $\alpha > 0.7$ is required for full 2-electron photoreduction. **PDI-1** is also monomeric in chloroform and dichloromethane (α is 0.62 and 0.68, respectively), but UVC

illumination leads to rapid photodegradation, yielding yellow solutions. Visual evidence of photoreduction and disassembly of **PDI-1$_{agg}$** comes from confocal microscopy, where we illuminate a circular region using a 355 nm UVB laser (60 mW), leading to rapid (~20 s) disappearance of colloidal aggregates and a ~80 nm blue shift of the emission spectrum (see Video S1), characteristic[39] for **PDI-1^{2-}**. It was previously shown that PDI aggregation makes chemical reduction easier,[39,40] since aggregation enhances charge delocalization and disproportionation of two PDI$^{\bullet-}$ into PDI and PDI^{2-} is possible. The same argumentation seems to hold for photoreduction of **PDI-1$_{agg}$** under vacuum conditions. So far, we have shown that photoreduction to **PDI-1^{2-}** is efficient under anaerobic conditions when starting from **PDI-1$_{agg}$** aggregates and having light with enough intensity and energy (i.e., UVB or UVC, >1 W/m^2).

In performing anaerobic photoreduction experiments of **PDI-1$_{agg}$** in different solvent mixtures, we noticed that even small quantities of acetone added to the buffer led to a great acceleration of **PDI-1^{2-}** production. This made us wonder whether the photoreduction might actually be faster than oxidation by oxygen even if the reaction were done in air. Indeed, even a stirred open cuvette containing 3 mL of **PDI-1$_{agg}$** solution (9% v/v acetone in buffer) could be reduced first to **PDI-1$^{\bullet-}$** and then to **PDI-1^{2-}** within 3 minutes (Figure 2A, 2× 8200 mW/m^2), which is very fast. Stopping the UV light leads to fast oxidation and recovery of the pink **PDI-1** color; restarting the UVC light again results in fast reduction (see Video 2). Figure 2B shows the red and blue color channels extracted from Video 2, where index i) shows the start of UVC light, ii) the maximum concentration of **PDI-1$^{\bullet-}$**, and iii) when **PDI-1^{2-}** is reached. Stopping the UVC LED just after index iii, resulted in oxidation from **PDI-1^{2-}** to **PDI-1$^{\bullet-}$** (see index iv in Figure 2B) and then to **PDI-1** in just ~1.5 minutes. Despite the possible photodamage (i.e. irreversible photochemical reaction) that can be caused by high energy UVC, the system studied herein is remarkably photostable even in air. Repeating the photoreduction/oxidation cycle 10 times did not lead to a reduction in response or any visible photobleaching of the system (Figure 2B). We believe acetone acts as a photocatalyst in our system as depicted in Figure 2C. The UVC light photoexcites acetone (first to singlet and then to triplet), which by electron transfer and/or H-abstraction from TEOA[41] produces the acetone ketyl radical anion Me$_2$(O$^-$)C$^\bullet$. The latter has a pK_a of 12,[42] so we expect ~6% of Me$_2$(O$^-$)C$^\bullet$ vs. ~94% of Me$_2$(OH)C$^\bullet$, which is a weaker reductant. The ketyl radical anion is a very good reductant in our system, and its electron is quickly scavenged by **PDI-1$_{agg}$** to eventually form **PDI-1^{2-}**, while at the same time regenerating acetone (Figure 2C). Under our conditions it is unlikely that pinacol is formed or that there is significant disproportionation of two ketyl radicals to acetone and isopropanol.[31] A control experiment replacing TEOA by isopropanol led to similar photoreduction rates, but also caused severe photobleaching (Figure S4), making it less practical for use in dissipative self-assembly systems.

Interestingly, assembly of **PDI-1** is not strictly required in the presence of acetone, since the photoreduction works in the monomeric state in DMF as well (see Figure S5). In addition,

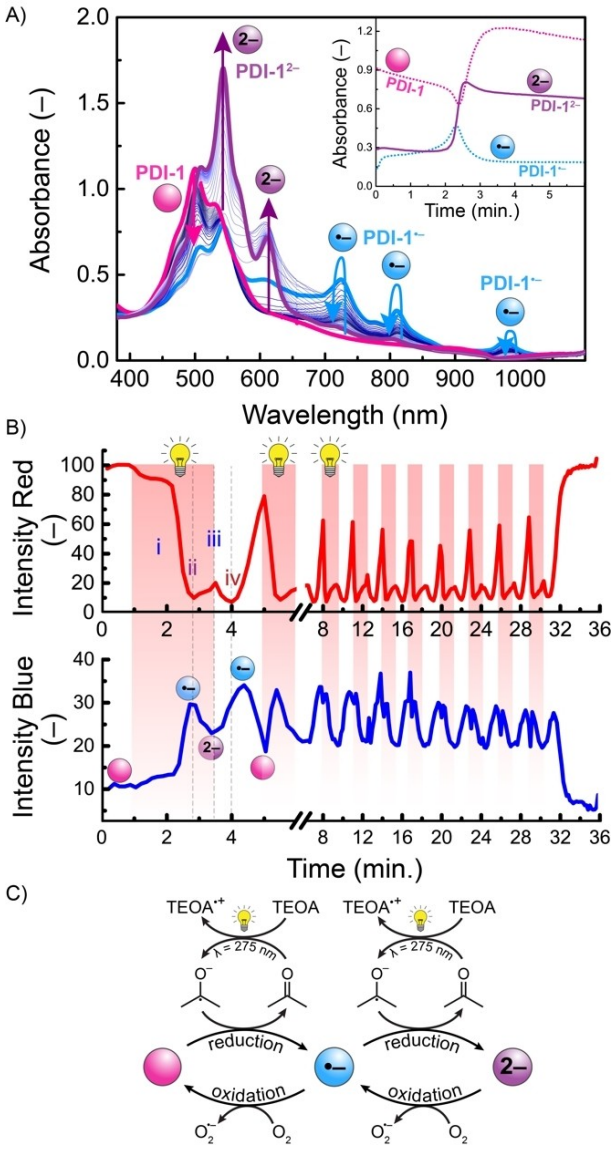

Figure 2. Acetone catalysed 'indirect photoreduction' under aerobic conditions (33 μM **PDI-1$_{agg}$** in buffer, 9% v/v acetone, 3000 eq. TEOA). A) UV-Vis spectra upon UVC illumination. The inset shows absorbances of **PDI-1$_{agg}$**, **PDI-1$^{\bullet-}$**, and **PDI-1^{2-}** 526, 725, and 543 nm, respectively. B) 10 photoredox cycles of **PDI-1** in buffer (2.25 mL, 50 μM, 3000 eq. of TEOA) under constant stirring to introduce O_2. Shaded salmon coloured areas shown when the UVC light is on. C) Acetone-catalyzed photoreduction mechanism (see main text).

also other aromatic dyes could be photoreduced, namely perylenediimide-alanine (**PDIA**), naphthalenediimide-aminoisophtalic acid (**NDI-PA**), and methyl viologen (**MV^{2+}**) as shown in Figure 3. All three molecules are photoreduced in ~1 minute in a 1×1 cm quartz cuvette that was not degassed or protected from air. Methyl viologen derivatives have been used to make supramolecular gels using cucurbituril guest–host complexation,[43,44] so combining this with efficient photoreduction would be an interesting strategy to obtain out-of-equilibrium materials in open air. Similarly for PDI or NDI-based materials, light-driven versions of current systems showing

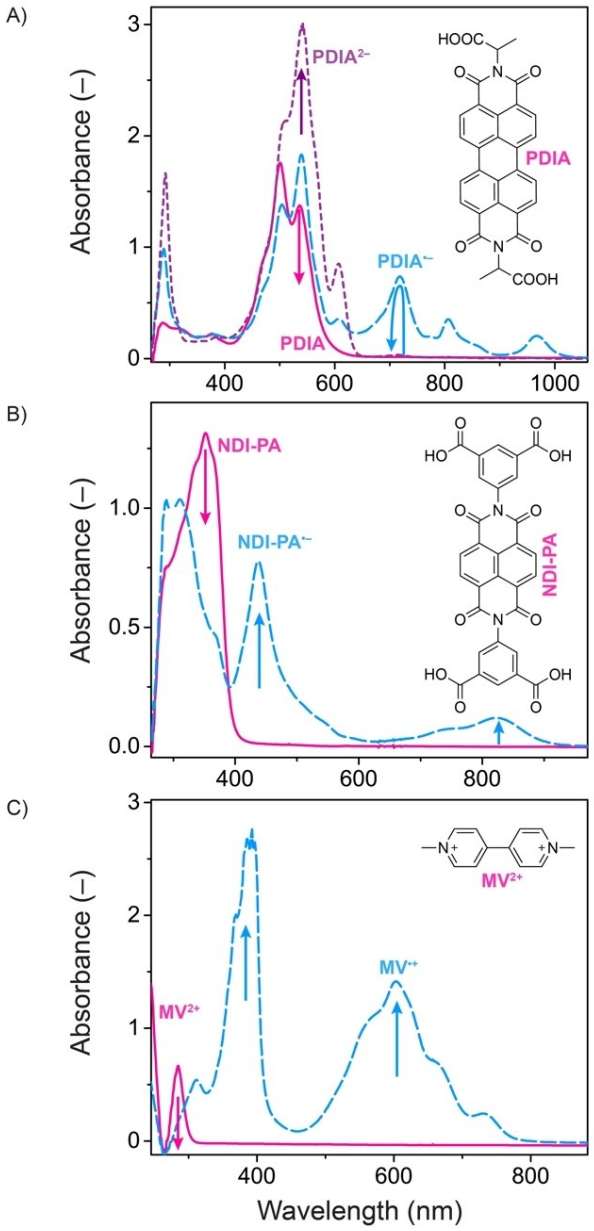

Figure 3. UV-Vis spectra of **PDIA**, **NDI-PA**, and $\mathbf{MV^{2+}}$ before and after irradiation with UVC LED light (open cuvette, 9% v/v acetone in carbonate buffer pH 10.8, 3000 eq. TEOA). A) **PDIA** (46.7 μM) shows fully reduced $\mathbf{PDIA^{2-}}$ after 43 s of UVC irradiation. B) **NDI-PA** (100 μM) after 34 s. C) $\mathbf{MV^{2+}}$ (134 μM) after 73 s.

supramolecular oscillations,[29] transient gels,[19] electrochromic gels,[45] or self-sorting polymerization[46] might be possible. Lastly, we show that 1,4-diazabicyclo[2.2.2]octane (DABCO) can be added to reduce photobleaching (see Figure S6), and thus increase the practical usability of this indirect photoreduction strategy.

Conclusions

In conclusion, we have shown both direct and indirect methods to achieve efficient photoreduction of PDIs and other aromatic dyes. When PDIs are self-assembled, $\mathbf{PDI\text{-}1^{2-}}$ can be quickly formed upon UVC irradiation under anaerobic conditions. The acetone catalyzed photoreduction proved to be very fast even in aqueous solutions that are not degassed or under protective atmosphere. The latter method works even for monomeric PDIs as well as for various types of dye molecules. This strategy will accelerate the development of a range of life-like materials based on photoredox cycles, with spatiotemporal control over where assembly and disassembly can occur.

Acknowledgements

CC, TMH, JSV acknowledge funding from ERC Starting Grant "Life-cycle" with grant number 757910.

Conflict of Interest

The authors declare no conflict of interest.

Data Availability Statement

The data that support the findings of this study are available from the corresponding author upon reasonable request.

Keywords: ketyl radical · perylenediimide · photoreduction · redox · self-assembly

[1] C. Jung, B. K. Müller, D. C. Lamb, F. Nolde, K. Müllen, C. Bräuchle, *J. Am. Chem. Soc.* **2006**, *128*, 5283–5291.
[2] X. Zhan, Z. Tan, E. Zhou, Y. Li, R. Misra, A. Grant, B. Domercq, X.-H. Zhang, Z. An, X. Zhang, S. Barlow, B. Kippelen, S. R. Marder, *J. Mater. Chem.* **2009**, *19*, 5794–5803.
[3] D. Schmidt, D. Bialas, F. Wurthner, *Angew. Chem. Int. Ed.* **2015**, *54*, 3611–3614; *Angew. Chem.* **2015**, *127*, 3682–3685.
[4] E. R. Draper, L. J. Archibald, M. C. Nolan, R. Schweins, M. A. Zwijnenburg, S. Sproules, D. J. Adams, *Chem. Eur. J.* **2018**, *24*, 4006–4010.
[5] E. R. Draper, J. J. Walsh, T. O. McDonald, M. A. Zwijnenburg, P. J. Cameron, A. J. Cowan, D. J. Adams, *J. Mater. Chem. C* **2014**, *2*, 5570–5575.
[6] A. Nowak-Król, B. Fimmel, M. Son, D. Kim, F. Würthner, *Faraday Discuss.* **2015**, *185*, 507–527.
[7] X. Li, N. Markandeya, G. Jonusauskas, N. D. McClenaghan, V. Maurizot, S. A. Denisov, I. Huc, *J. Am. Chem. Soc.* **2016**, *138*, 13568–13578.
[8] C. Piliego, D. Jarzab, G. Gigli, Z. Chen, A. Facchetti, M. A. Loi, *Adv. Mater.* **2009**, *21*, 1573–1576.
[9] M. Bonchio, Z. Syrgiannis, M. Burian, N. Marino, E. Pizzolato, K. Dirian, F. Rigodanza, G. A. Volpato, G. La Ganga, N. Demitri, S. Berardi, H. Amenitsch, D. M. Guldi, S. Caramori, C. A. Bignozzi, A. Sartorel, M. Prato, *Nat. Chem.* **2019**, *11*, 146–153.
[10] Y. Xu, J. Zheng, J. O. Lindner, X. Wen, N. Jiang, Z. Hu, L. Liu, F. Huang, F. Würthner, Z. Xie, *Angew. Chem. Int. Ed.* **2020**, *59*, 10363–10367; *Angew. Chem.* **2020**, *132*, 10449–10453.
[11] L. Cui, Y. Jiao, A. Wang, L. Zhao, Q. Dong, X. Yan, S. Bai, *Chem. Commun.* **2018**, *54*, 2208–2211.
[12] H. Wang, K.-F. Xue, Y. Yang, H. Hu, J.-F. Xu, X. Zhang, *J. Am. Chem. Soc.* **2022**, *144*, 2360–2367.

[13] B. Lü, Y. Chen, P. Li, B. Wang, K. Müllen, M. Yin, *Nat. Commun.* **2019**, *10*, 767.
[14] Y. Yang, P. He, Y. Wang, H. Bai, S. Wang, J.-F. Xu, X. Zhang, *Angew. Chem. Int. Ed.* **2017**, *56*, 16239–16242; *Angew. Chem.* **2017**, *129*, 16457–16460.
[15] I. Ghosh, T. Ghosh, J. I. Bardagi, B. Konig, *Science* **2014**, *346*, 725–728.
[16] L. Zeng, T. Liu, C. He, D. Shi, F. Zhang, C. Duan, *J. Am. Chem. Soc.* **2016**, *138*, 3958–3961.
[17] M. Marchini, A. Gualandi, L. Mengozzi, P. Franchi, M. Lucarini, P. G. Cozzi, V. Balzani, P. Ceroni, *Phys. Chem. Chem. Phys.* **2018**, *20*, 8071–8076.
[18] J. Leira-Iglesias, A. Sorrenti, A. Sato, P. A. Dunne, T. M. Hermans, *Chem. Commun.* **2016**, *52*, 9009–9012.
[19] E. Krieg, E. Shirman, H. Weissman, E. Shimoni, S. G. Wolf, I. Pinkas, B. Rybtchinski, *J. Am. Chem. Soc.* **2009**, *131*, 14365–14373.
[20] R. Renner, M. Stolte, J. Heitmüller, T. Brixner, C. Lambert, F. Würthner, *Mater. Horiz.* **2022**, *9*, 350–359.
[21] S. K. Mohan Nalluri, J. Zhou, T. Cheng, Z. Liu, M. T. Nguyen, T. Chen, H. A. Patel, M. D. Krzyaniak, W. A. Goddard, M. R. Wasielewski, J. F. Stoddart, *J. Am. Chem. Soc.* **2019**, *141*, 1290–1303.
[22] Y. Song, W. Zhang, S. He, L. Shang, R. Ma, L. Jia, H. Wang, *ACS Appl. Mater. Interfaces* **2019**, *11*, 33676–33683.
[23] D. Gosztola, M. P. Niemczyk, W. Svec, A. S. Lukas, M. R. Wasielewski, *J. Phys. Chem. A* **2000**, *104*, 6545–6551.
[24] D. Schmidt, D. Bialas, F. Wurthner, *Angew. Chem. Int. Ed.* **2015**, *54*, 3611–4; *Angew. Chem.* **2015**, *127*, 3682–3685.
[25] S. Seifert, D. Schmidt, F. Wurthner, *Chem. Sci.* **2015**, *6*, 1663–1667.
[26] N. T. La Porte, J. F. Martinez, S. Hedström, B. Rudshteyn, B. T. Phelan, C. M. Mauck, R. M. Young, V. S. Batista, M. R. Wasielewski, *Chem. Sci.* **2017**, *8*, 3821–3831.
[27] H. Li, O. S. Wenger, *Angew. Chem. Int. Ed.* **2022**, *61*, e202110491.
[28] X. Zhan, A. Facchetti, S. Barlow, T. J. Marks, M. A. Ratner, M. R. Wasielewski, S. R. Marder, *Adv. Mater.* **2011**, *23*, 268–284.
[29] J. Leira-Iglesias, A. Tassoni, T. Adachi, M. Stich, T. M. Hermans, *Nat. Nanotechnol.* **2018**, *13*, 1021–1027.
[30] R. Klajn, *Chem* **2021**, *7*, 23–37.
[31] H. C. A. van Beek, P. M. Heertjes, K. Schaafsma, *J. Soc. Dyers Colour.* **1971**, *87*, 342–348.
[32] H. C. A. van Beek, P. M. Heertjes, C. Houtepen, D. Retzloff, *J. Soc. Dyers Colour.* **1971**, *87*, 87–92.
[33] R. Flyunt, W. Knolle, A. Kahnt, C. E. Halbig, A. Lotnyk, T. Häupl, A. Prager, S. Eigler, B. Abel, *Nanoscale* **2016**, *8*, 7572–7579.
[34] F. Würthner, Z. Chen, V. Dehm, V. Stepanenko, *Chem. Commun.* **2006**, 1188–1190.
[35] Z. Chen, B. Fimmel, F. Würthner, *Org. Biomol. Chem.* **2012**, *10*, 5845–5855.
[36] A. D. Shaller, W. Wang, A. Li, G. Moyna, J. J. Han, G. L. Helms, A. D. Q. Li, *Chem. Eur. J.* **2011**, *17*, 8350–8362.
[37] A. D. Shaller, W. Wang, A. Li, G. Moyna, J. J. Han, G. L. Helms, A. D. Q. Li, *Chem. Eur. J.* **2011**, *17*, 8350–8362.
[38] J. Gershberg, F. Fennel, T. H. Rehm, S. Lochbrunner, F. Würthner, *Chem. Sci.* **2016**, *7*, 1729–1737.
[39] E. Shirman, A. Ustinov, N. Ben-Shitrit, H. Weissman, M. A. Iron, R. Cohen, B. Rybtchinski, *J. Phys. Chem. B* **2008**, *112*, 8855–8858.
[40] R. O. Marcon, S. Brochsztain, *J. Phys. Chem. A* **2009**, *113*, 1747–1752.
[41] Á. Péter, S. Agasti, O. Knowles, E. Pye, D. J. Procter, *Chem. Soc. Rev.* **2021**, *50*, 5349–5365.
[42] G. P. Laroff, R. W. Fessenden, *J. Phys. Chem.* **1973**, *77*, 1283–1288.
[43] Z. Yin, G. Song, Y. Jiao, P. Zheng, J.-F. Xu, X. Zhang, *CCS Chemistry* **2019**, *1*, 335–342.
[44] J. Liu, C. S. Y. Tan, O. A. Scherman, *Angew. Chem. Int. Ed.* **2018**, *57*, 8854–8858; *Angew. Chem.* **2018**, *130*, 8992–8996.
[45] L. Gonzalez, C. Liu, B. Dietrich, H. Su, S. Sproules, H. Cui, D. Honecker, D. J. Adams, E. R. Draper, *Commun. Chem.* **2018**, *1*, 77.
[46] M. Hecht, P. Leowanawat, T. Gerlach, V. Stepanenko, M. Stolte, M. Lehmann, F. Würthner, *Angew. Chem.* **2020**, *132*, 17232–17238; *Angew. Chem. Int. Ed.* **2020**, *59*, 17084–17090.

Manuscript received: September 13, 2022
Accepted manuscript online: September 16, 2022
Version of record online: November 10, 2022